Reevaluating the Canyon Hypothesis in a Biological Hotspot in the Western Antarctic Peninsula

K. Hudson[1] [iD], M. J. Oliver[1] [iD], K. Bernard[2] [iD], M. A. Cimino[3] [iD], W. Fraser[4], J. Kohut[5] [iD], H. Statscewich[6] [iD], and P. Winsor[6]

[1]College of Earth, Ocean, and Environment, University of Delaware, Lewes, DE, USA, [2]College of Earth, Ocean, and Atmospheric Sciences, Oregon State University, Corvallis, OR, USA, [3]Institute of Marine Science, University of California, Santa Cruz, CA, USA, [4]Polar Oceans Research Group, Sheridan, MT, USA, [5]Department of Marine and Coastal Sciences, Rutgers, The State University of New Jersey, New Brunswick, NJ, USA, [6]College of Fisheries and Ocean Sciences, University of Alaska Fairbanks, Fairbanks, AK, USA

Abstract In the Western Antarctic Peninsula, increased biological activity at many levels of the food web are spatially coherent with submarine canyons. One possible mechanism that links the presence of these canyons to increased biological productivity is through the local upwelling of nutrient-rich modified Upper Circumpolar Deep Water (mUCDW) to the surface, which supports high phytoplankton stocks, krill, penguins, and whales. In the austral summer of 2015, we investigated this hypothesis by deploying three autonomous Slocum gliders over Palmer Deep Canyon, near Palmer Station, Antarctica. Although we observed the shallowing of mUCDW consistent with canyon-driven isopycnal uplift, these deep waters did not penetrate the phytoplankton rich surface mixed layer. Waters below the mixed layer, however, were strongly coherent with bathymetry, suggesting the strong influence of the canyon. The decoupling of the surface mixed layer from the mUCDW suggests that local upwelling may not be the mechanism that supports the biological hotspot. New physical mechanisms that could support the biological hotspot at Palmer Deep Canyon are suggested.

Plain Language Summary It has been suggested that the association of deep submarine canyons and the biological hotspot at Palmer Deep Canyon in the Western Antarctic Peninsula is due to the local upwelling of deep, nutrient-rich water to the surface, increasing phytoplankton growth and thus attracting local krill and, in turn, supporting upper trophic levels. However, we found that during the season of peak biological activity, summer stratification isolates the productive surface waters from the nutrient-rich water. Therefore, we suggest that upwelling of nutrient-rich water is not the mechanism driving this canyon associated biological hotspot. We suggest alternative mechanisms related to horizontal transport.

1. Introduction

Submarine canyons that traverse the continental shelf and terminate within a few kilometers of the shore in the Western Antarctic Peninsula (WAP) are often considered biological hotspots due to their association with high biological activity (Carvalho et al., 2016; Fraser & Trivelpiece, 1996; Kavanaugh et al., 2015; Schofield et al., 2013). Adélie, gentoo, and chinstrap penguin colonies, some of which have persisted across millennial time scales (Emslie & Patterson, 2007), are often present at the terminus of these canyons. This has become the foundational observation for the "canyon hypothesis," which suggests that there is a mechanistic relationship between these biological hotspots and the presence of these canyons (Fraser & Trivelpiece, 1996; Schofield et al., 2013). One suggested mechanism linking the presence of these hotspots to the canyons is the upwelling of nutrient-rich Upper Circumpolar Deep Water (UCDW) that would, in theory, support the growth of phytoplankton, Antarctic krill, and their upper level trophic predators (Prézelin et al., 2000). Indeed, the source of nutrient-rich waters along the WAP is likely the result of UCDW intrusions at the continental shelf break (Smith et al., 1999) that are transported across the continental shelf via subsurface eddies and canyons (Couto, Martinson, et al., 2017). Prézelin et al. (2000) suggested that the upwelling of UCDW at the shelf break could provide a dependable food source within penguins' 100- to 150-km foraging range (Fraser & Trivelpiece, 1996; see inset of Figure 1 for region studied by Prézelin et al., 2000). However, satellite telemetry of Adélie penguins in this region show that they rarely venture
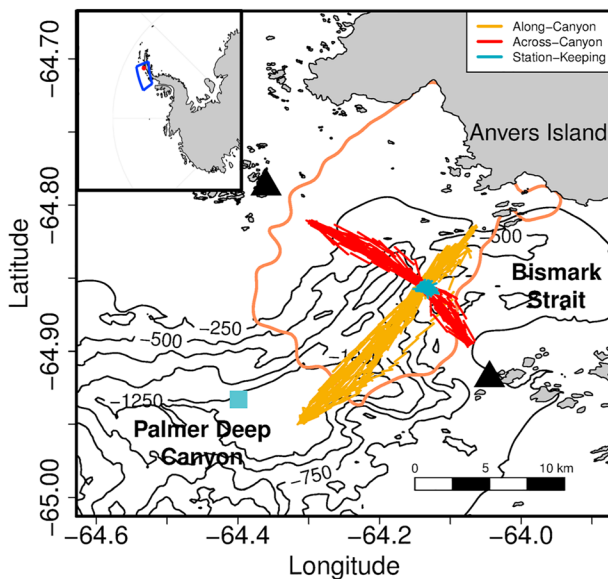
Figure 1. Bathymetry map of Palmer Deep Canyon with the tracks of three Slocum gliders used in this analysis. The inset illustrates the Western Antarctic Peninsula, with the red dot representing the location of Palmer Deep Canyon and the blue box illustrating the study region where Prézelin et al. (2000) described outer-shelf upwelling in the Western Antarctic Peninsula. Bathymetry is from Global Multiresolution Topography (Ryan et al., 2009). The light blue square represents Station 600-040 within the Palmer Long Term Ecological Research sampling grid. The coral line represents the 99.5% contour for Adélie penguin foraging locations for penguins tagged between 2002 and 2011. Black triangles represent the two weather stations where wind data were collected.

to these offshore upwelling sites but rather stay within approximately 20 km of their colony (Oliver et al., 2013; Pickett et al., 2018; Oliver et al., 2019), even though the shelf break upwelling sites are within their known foraging range (Fraser & Trivelpiece, 1996). It is certainly possible that shoreward horizontal transport of production from the offshore upwelling sites could benefit upper trophic level species in their nearshore foraging habitats. However, the observation that Adélie penguin foraging is restricted to the canyons near their colonies has led ecologists and oceanographers to clarify and reduce the length scales of the potential mechanisms driving the observed hotspots.

Palmer Deep Canyon (PDC) biological hotspot, located off the southern shore of Anvers Island in the WAP, is believed to be related to the local shoaling of warm, nutrient-rich UCDW (Schofield et al., 2013) at the nearshore canyon terminus. A multiyear analysis of satellite chlorophyll, temperature, and sea ice over PDC showed higher chlorophyll concentrations over the canyon compared to nearby coastal regions (Kavanaugh et al., 2015). Importantly, the distance between canyon and noncanyon sites in this analysis was ~10 km, which is on the same scale as the penguin foraging range in PDC. A localized UCDW upwelling signal within PDC could explain the consistently higher satellite-derived chlorophyll concentrations, consistently lower sea ice cover, and restricted foraging range of Adélie penguins in January and February (Kavanaugh et al., 2015). These observations provide strong circumstantial evidence that local upwelling is the mechanism that spurs increased biological activity in PDC during the middle to late summer months.

This localized view of the upwelling mechanism that supports this hotspot has several key assumptions. The first is that nutrient-rich UCDW penetrates the lighted surface layer where it can be utilized by phytoplankton. The second is that the lighted surface layer is nutrient-limited, and the upwelling of nutrient-rich UCDW to this layer supplies the necessary nutrients for phytoplankton growth. The third is that the residence time of this surface layer is long enough for phytoplankton biomass to respond to these upwelled nutrients and accumulate through growth. The fourth is that the increased phytoplankton biomass attracts krill, which in-turn support upper trophic predators such as penguins. While local upwelling has been suggested as the mechanism that supports PDC biological hotspot, there have been few direct observations of upwelling. For example, using a single buoyancy-driven Slocum glider, Schofield et al. (2013) reported that nutrient-rich UCDW was shoaling within PDC. However, it was unclear if the event promoted biological productivity within the canyon system or if the event was persistent enough to support the hypothesis that continuous upwelling within PDC drives the biological hotspot.

Here we use three buoyancy-driven Slocum gliders to test the canyon hypothesis and observe local upwelling events of UCDW within PDC in January and February of 2015 during the seasonal peak of biological activity. We hypothesize that these upwelling events are the mechanism driving the biological hotspot in PDC. Gliders have become a standard platform for oceanographic research; however, their relatively slow transit speeds often make it difficult to discern if the changes observed along a transect are due to conditions changing in time or space. We attempted to address this issue by deploying two gliders in a cross pattern, with a third glider holding station at their intersection. We used the differences in these transects to discern which mechanisms likely drive differences throughout the canyon above and below the mixed layer.

2. Methods

2.1. Glider Data Collection

Three Slocum electric gliders were used to collect the physical and biological data used to describe the oceanography of PDC. One glider ran a transect across PDC, parallel to the coast of Anvers Island; another ran a transect along PDC, perpendicular to the coast of Anvers Island; and the third glider held station at the

intersection of the other two glider transects (Figure 1) near the head of the canyon. Two of these gliders (station-keeping and across-canyon) sampled the upper 100 m of the water column, while the third (along-canyon) sampled the upper 200 m.

All three gliders were deployed on 5 January 2015. The station-keeping and across-canyon vehicles were recovered and redeployed after battery replacement during the month of January. Since the decorrelation analysis (section 2.3) assumes a continuous time series, the glider missions were separated into two sequential field experiments when all three gliders were on their assigned lines (Figure 1). The station-keeping glider completed 1,249 profiles during the first experiment and 1,684 profiles during the second experiment. The along-canyon glider completed 608 and 807 profiles during the first and second experiments, respectively. The across-canyon glider completed 791 profiles during the first experiment and 1,148 profiles during the second experiment. We treated these experiments independently for all analyses described below.

The sampling methods and configurations of the three gliders are described in Kohut et al. (2014). In brief, each glider was equipped with a SeaBird conductivity, temperature, and depth (CTD) and Wet Labs Eco Triplet fluorometer that sampled approximately every 0.5 m. The Wet Labs Eco Triplet was configured to measure backscatter in addition to chlorophyll *a* concentration. Only data from the downcasts were used because science sensors were sometimes turned off on upcasts to save power. Data from these gliders were cross-calibrated using data from when they were in close proximity at the station-keeping location (supporting information Text S1, equations S1–S4, and Figure S1). These relationships were used to correct the complete data set.

The gliders estimated depth-integrated water currents between surface events by comparing surface GPS locations with dead-reckoning subsurface navigation (Schofield et al., 2007). Mixed layer depth (MLD) was derived using the methods of Carvalho et al. (2016), which is based on the depth of the maximum buoyancy frequency (Carvalho et al., 2017). Wind and bathymetry data were also matched to glider data. Wind was measured at the Joubin and Wauwermans Islands weather stations, and bathymetry data are from ETOPO1. The bathymetry was matched to glider data at its native resolution.

2.2. Water Mass Identification

Water masses observed during these experiments were identified using the temperature and salinity definitions from Carvalho et al. (2016) after analyzing six field seasons (2010–2015) with 26,455 upper water column profiles. Carvalho et al. (2016) defined modified UCDW (mUCDW) as water with temperatures between 0 and 1 °C and a salinity range between 34.1 and 34.7. Winter Water (WW) was defined as water with a temperature equal to or less than −1.2 °C and salinities between 33.85 and 34.13. Surface waters, also known as Antarctic (summer) Surface Water (AASW), were defined as waters having temperatures between 0 and 4 °C and salinities between 32.5 and 33.5 (Carvalho et al., 2016; Smith et al., 1999).

2.3. Decorrelation Analysis

Depth-resolved glider data were separated into 10-m depth bins across the three gliders and two experiments. To examine the differences between the mixed layer and deeper water masses such as mUCDW, we focused on the 0- to 10-m and 80- to 90-m bins. The 0- to 10-m bin was used because it was consistently within the mixed layer throughout both experiments. The 80- to 90-m bin was chosen because it was well below the mixed layer.

Within each depth bin, the data were linearly interpolated to hourly time stamps using the function *approx* in the *zoo* package in R (R Core Team, 2017). These data were used to perform a decorrelation analysis for each glider and depth bin. Decorrelations were detrended using the *acf* function in the *stats* package in R. The mean was removed from each time series, and the maximum lag was set to 80 hr to encompass the time it took for the across- and along-canyon gliders to complete two transects. Daily trends were not removed from surface data to avoid removing episodic surface events. Equation (1) calculates the 95% confidence intervals for complete decorrelation.

$$95\%\mathrm{CI} = \pm \frac{\frac{1.95}{2}}{\sqrt{\text{length of time series}}} \qquad (1)$$

Decorrelation analysis assumes that the data are Eulerian, meaning that data are collected at the same location throughout the time series. Therefore, we attributed differences between the station-keeping and along- and across-glider correlations to spatial differences along the transects in PDC, both at the surface and at depth.

2.4. Historical LTER data

Historic data from the Palmer Long Term Ecological Research (LTER) program were accessed from the Palmer LTER website (https://oceaninformatics.ucsd.edu/datazoo/catalogs/pallter/datasets). We used CTD (Iannuzzi, 2018), nutrient, and light irradiance data (Ducklow et al., 2019) from the annual Palmer LTER cruises between 1993 and 2018 during the summer months (December–February). Station 600-040 within the sampling grid is over PDC and Station 600-080 is located 40 km to the northwest, outside of PDC (Figures 1 and S2). Sampling frequency varied between the stations. At Station 600-040, CTD data were collected every year between 1993 and 2017, and nutrient profiles were collected every year from 1993 to 2018. Light percent irradiance was collected at Station 600-040 in 1998–2000, 2002–2003, and 2005–2008. At Station 600-080, CTD casts were conducted between 1993 and 2008 and in 2014. Nutrient profiles were conducted in 1995–1996, 1999, and 2000–2008.

CTD and nutrient data were averaged across sampling years. CTD data were binned in 10-m depth bins. Nutrient data were binned in 10-m depth bins above 50- and 50-m bins at deeper depths to account for lower vertical resolution in the data. Percent light irradiance was averaged by year and in 5-m depth bins for the 9 years between 1998 and 2008 (1998–2000, 2002–2003, and 2005–2008) where irradiance data were available to estimate the depth of the euphotic zone (1% light level).

## 3. Results

3.1. Glider Observations of PDC

In the austral summer of 2015, PDC was stratified with a warm, relatively fresh surface layer that deepened and became less fresh as the season progressed (Figures 2 and S3–S5). The MLD begins to deepen from a mean of 13.5 m during the first experiment to a mean of 32 m during the second experiment in all transects on 23 January, which is coincident with a large wind event, reaching an hourly maximum of 15 m/s with a mean speed of 7 m/s on that day. The deepening of the MLD around 5 February to a mean of 44 m between 5 and 7 February was also coincident with high, sustained hourly winds on 5 February, with mean wind speeds of 11 m/s (Figure 2a). This resulted in an increase in the surface layer density between the first and second experiments (Figure S4).

A cool water mass was observed below the MLD. This water mass had a mean temperature of approximately 0 °C and mean salinity of approximately 33.5 (Figures 2, S3, and S5), which was likely remnant WW, carrying the thermal signature from the previous winter, but distinct from the surface layer due to seasonal warming (Carvalho et al., 2016). As the MLD deepened further into the summer, the thickness of the WW decreased from ~25 to ~12 m (Figures 2, S3, and S4). The thickness of the WW was greater in the station-keeping and across-canyon observations than in the along-canyon observations (Figures 2, S3, and S4), especially in the second experiment when the MLD deepened (Figures 2, S3, and S4).

A distinct water mass was observed below the WW (Figures 2 and S3–S5). This water mass had a temperature range between 0.5 °C at the upper edge and 1.25 °C at 200 m (Figures 2 and S5). The salinity of this layer ranged between 34.25 at the upper edge and 34.5 below 100 m (Figures S3 and S5). Based on our definitions, this water mass was mUCDW, which is a modified form of the UCDW water that has been hypothesized to be a source of upwelled nutrients for PDC (Kavanaugh et al., 2015).

The thickness of the WW layer was coherent with the bathymetry in the along-canyon transect, especially as the season progressed into February (Figures 2, S3, and S4). Thicker WW layers were found over shallower ocean depths (<500 m), while mUCDW was closer to the surface over deeper waters (>800 m; Figures 2, 3, S3, and S4). A thicker WW layer was found on the west side of the canyon, which is consistent with
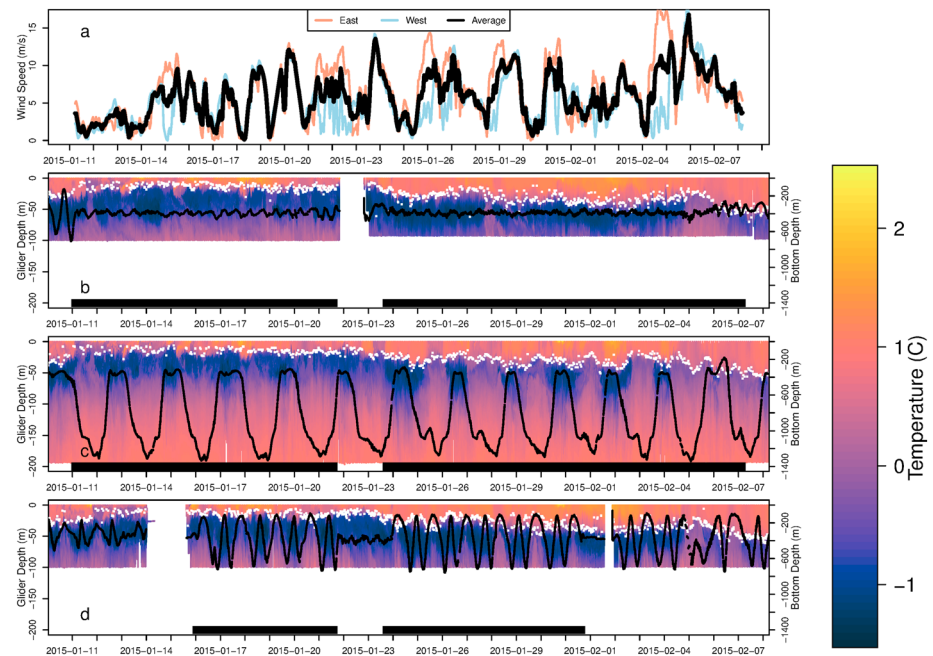
Figure 2. Wind speed across Palmer Deep Canyon (a) and temperature profiles collected by the station-keeping (b), along-canyon (c), and across-canyon (d) glider transects for both experimental periods. The bathymetry of Palmer Deep Canyon along the glider track is denoted by the black line and corresponds to the right *y* axis. Mixed layer depth is represented by the white dots and corresponds to the left *y* axis. The black bars along the *x* axis denote the two time periods used for the two experiments. These times correspond to when all three gliders were deployed along their respective transects.
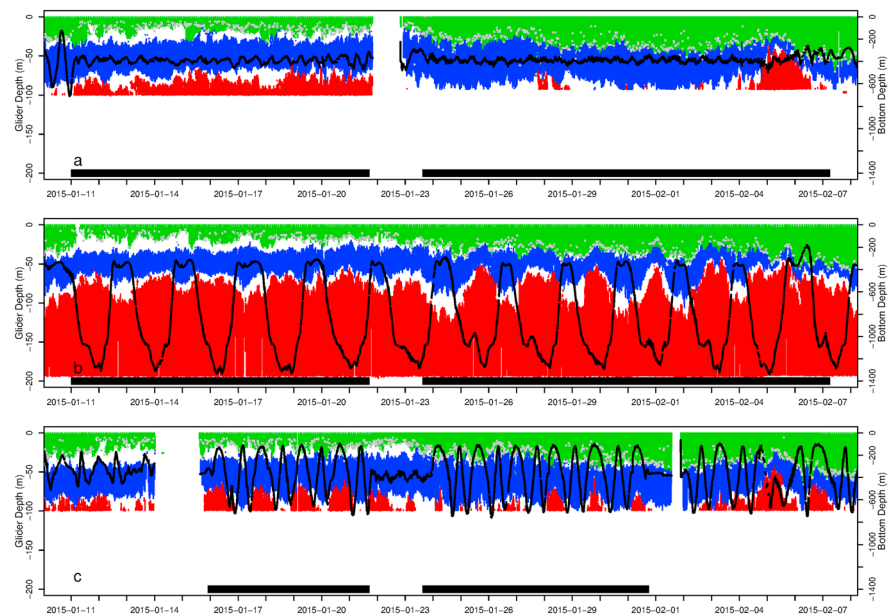

Figure 3. Distribution of Antarctic Surface Water (green), Winter Water (blue), and modified Upper Circumpolar Deep Water (red) water masses observed by the stationary (a), along-canyon (b), and across-canyon (c) glider transects during both experimental periods. The bathymetry of Palmer Deep Canyon along the glider track is denoted by the black line and corresponds to the right *y* axis. Mixed layer depth is represented by the gray dots and corresponds to the left *y* axis. The black bars along the *x* axis denote the two time periods used for the two experiments in the analysis of each glider. These times correspond to when all three gliders were deployed along their respective transects.
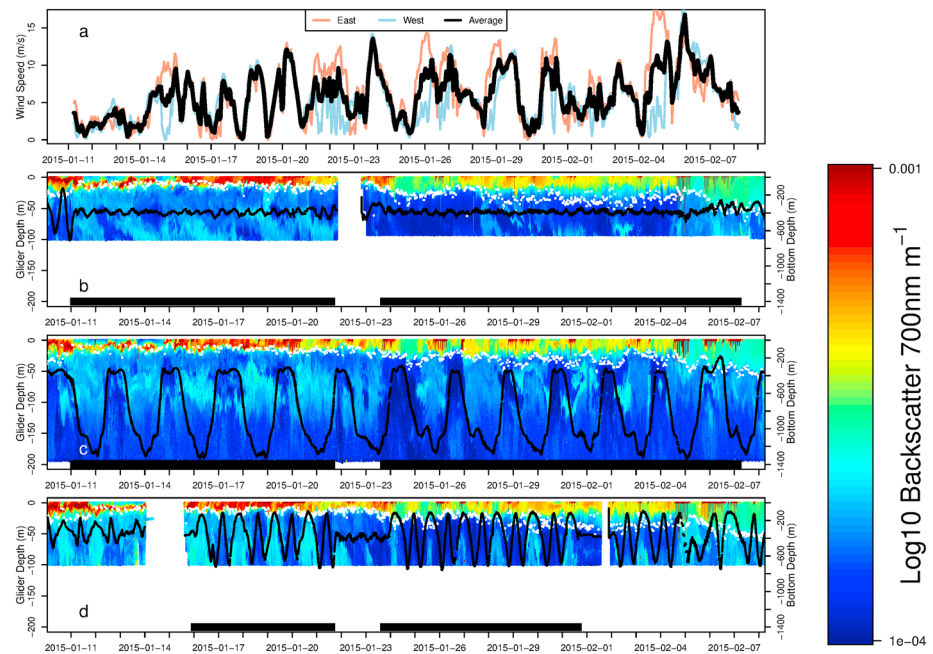
Figure 4. As in Figure 2 but with optical backscatter at 700 nm.

observations made by Carvalho et al. (2016) using six seasons of glider data from PDC (Figures S6a, S6b, S7a, and S7b). WW is a persistent feature during the summer months within PDC. WW was found in 87.5% of the 93 CTD profiles taken from Station 600-040 within the LTER sampling grid during the summer months from 1991 to 2017. WW in these profiles was found between 36 and 51 m deep on average. mUCDW was present in 93.8% of these CTD profiles, between 86 and 704 m on average. This pattern of WW and mUCDW distribution is evident in the transect-averaged properties in both experiments (Figures S6–S9). Therefore, we believe that 2015 was a representative year within PDC in terms of water mass structure.
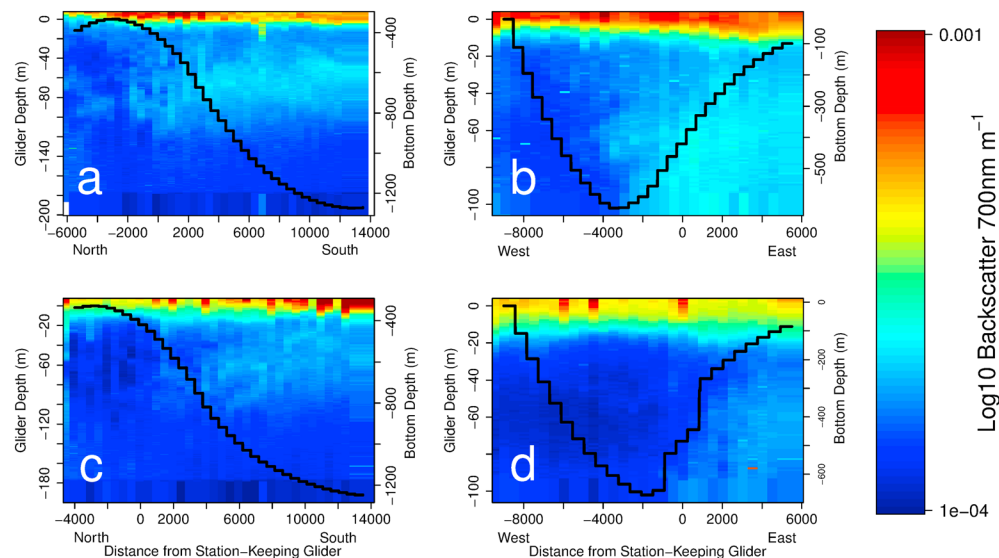
Figure 5. Average observations of optical backscatter from the along- (a,c) and across-canyon (b,d) transects during the first (a,b) and second (c,d) experiments. Observations were averaged on 0.5-km resolution. The black line denotes the average canyon depth experienced by the glider and corresponds to the right *y* axis in each panel.
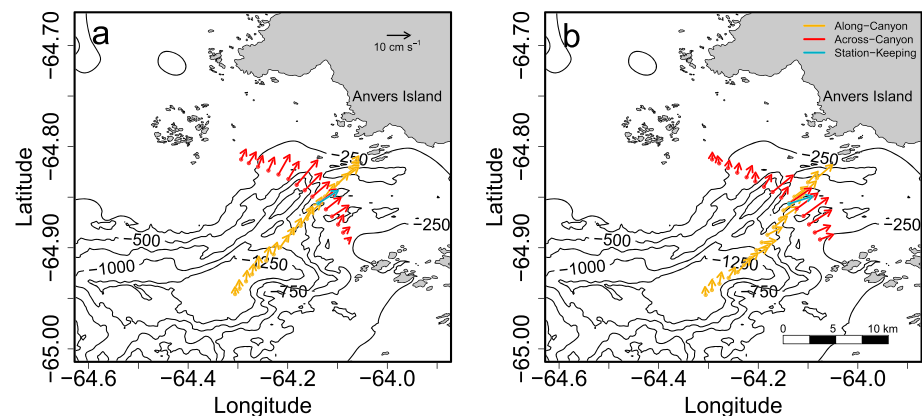
Figure 6. Integrated current velocity and direction in 1-km bins for each of the three glider transects during the first (a) and second (b) experiments. Thin black lines illustrate Palmer Deep Canyon bathymetry from Global Multiresolution Topography (Ryan et al., 2009).

Water mass vertical distributions across the two experiments showed that the depth of the AASW and thickness of the WW were strongly related to the MLD. As the season progressed, WW slowly eroded. During the first experiment, mUCDW stayed far below the mixed layer, with no obvious intrusions into the surface, as the WW formed a barrier between the mUCDW and AASW (Figure 3). This was true even during a strong wind event on 5–6 February in the second experiment (Figures 3a and 3b). However, in the second experiment, mUCDW became deeper in shallower portions of the canyon and shallower in deeper portions in the canyon (Figure 3b), coming closer to the mixed layer as the season progressed. This observation is consistent with the physical upwelling and doming of isopycnals in submarine canyons (Klinck, 1989; Mackas et al., 1997). This doming was more pronounced later in the season. There is also a strong across-canyon asymmetry of mUCDW (Figure 3c), which was also seen in the averaged across-canyon transects (Figures S6 and S7). Average temperature and salinity transects across the canyon indicated mUCDW was shallower on the east side of the canyon in both experiments (Figures S6a, S6b, S7a, and S7b).

Water spiciness (McDougall & Krzysik, 2015; Schmitt, 1999) was calculated as a proxy for potential cross isopycnal mixing (Figure S10). In short, higher water spice indicates warmer, saltier water, while decreased spice indicates colder, fresher water masses. The stratification, similar to that seen in the temperature, salinity, and density time series (Figures 2, S3, and S4), apparent in the time series of water spiciness indicates that there was minimal cross isopycnal mixing, with the exception of the wind driven mixing events described above (Figure S10).

Table 1
Decorrelation Time Scales of Temperature, Salinity, Chlorophyll, Backscatter, Current Velocity, MLD, and Wind Speed in Hours Observed in All Three Glider Transects at Shallow (0–10 m) and Deep (80–90 m) Depths During Both Experiments

| | Decorrelation time scales (hr) | | | | | |
| | Station-keeping | | Along-canyon | | Across-canyon | |
Variable	0–10 m	80–90 m	0–10 m	80–90 m	0–10 m	80–90 m
Temperature	25 (50)	15 (40)	40 (15)	12.5 (15)	25 (10)	8 (10)
Salinity	15 (7.5)	15 (40)	10 (15)	10 (15)	10 (10)	8 (10)
Chlorophyll	5 (10)	10 (18)	5 (10)	15 (15)	5 (10)	2.5 (5)
Backscatter	7.5 (2.5)	10 (18)	5 (2)	15 (15)	2.5 (1)	5 (10)
Current velocity	5 (5)		5 (5)		5 (5)	
MLD	5 (20)		5 (15)		10 (5)	
Wind speed	10 (10)		10 (15)		10 (10)	

Note. Decorrelations from the second experiment are in parentheses. Current velocity, MLD, and wind speed were not grouped by depth bin. MLD = mixed layer depth.
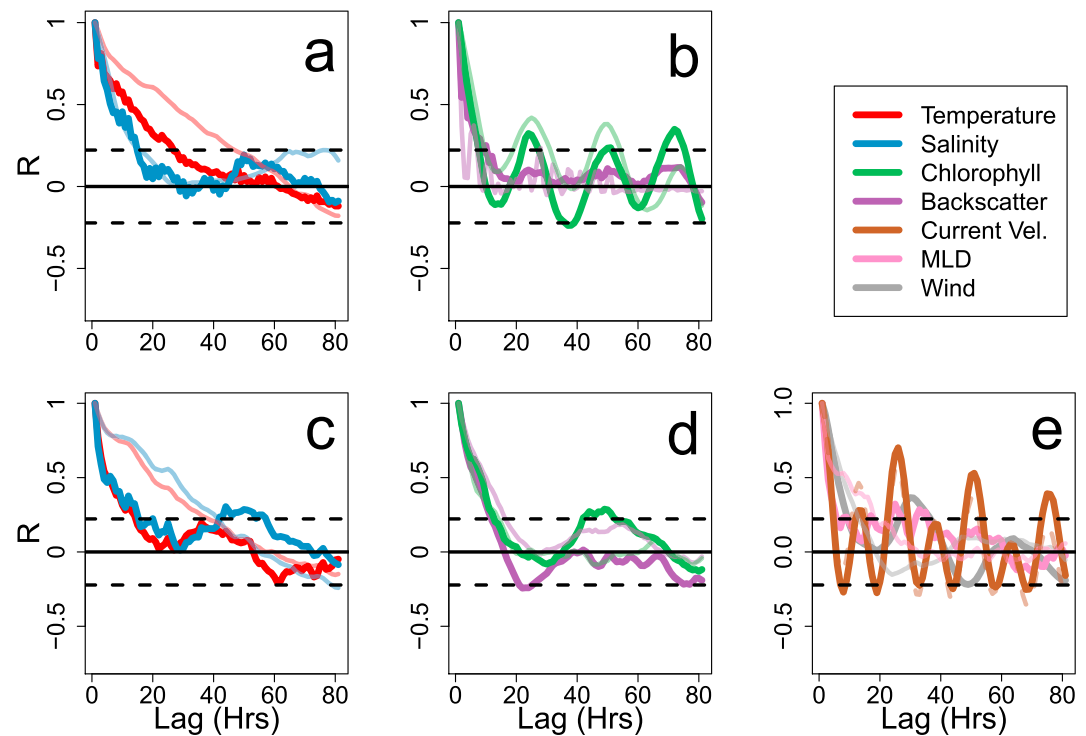
Figure 7. Decorrelations of temperature, salinity, chlorophyll, backscatter, current velocity, mixed layer depth (MLD), and wind speed from the station-keeping glider. Solid lines represent decorrelations during the first experiment, and translucent lines represent decorrelations during the second experiment. (a,b) Decorrelations in the surface layer between 0 and 10 m and (c,d) decorrelations in the deep layer between 80 and 90 m. (e) Current velocity, MLD, and wind speed did not change with depth. Dashed lines represent the 95% confidence intervals for zero correlation.

High chlorophyll concentrations and backscatter were observed in the AASW, across all transects (Figures 4 and S11). These high chlorophyll and backscatter observations deepened as the MLD deepened (Figures 4 and S11). Chlorophyll in the surface layer followed a diurnal nonphotochemical quenching (NPQ) pattern (Figure S11). Model II regressions of chlorophyll concentrations and backscatter above the MLD were highly correlated at night for all three gliders (Stationary, $R^2 = 0.91$; Along Canyon, $R^2 = 0.89$; Across Canyon, $R^2 = 0.81$) indicating that backscatter is also a good indicator of chlorophyll biomass and that NPQ explains the daily surface reductions in chlorophyll biomass.

Below the mixed layer, the along-canyon and across-canyon gliders showed elevated backscatter values in the deeper and the eastern portions of the canyon, possibly reflecting either particle export or particle retention from surface waters (Figures 5a, 5b, and S6–S9). These patterns persisted, but particle concentrations decreased in the second experiment (Figures 5c and 5d).

Glider-estimated current velocities averaged for each experiment were integrated from the surface to the maximum profiling depth and binned to every kilometer across each glider's respective transects (Figure 6). The station-keeping and across-canyon gliders had higher depth-integrated velocities than the along-canyon glider. This likely reflects the different glider dive depths and survey locations. The station-keeping and across-canyon gliders profiled to ~100 m, while the along-canyon glider profiled to ~200 m.

The mean flow in the upper water column observed across both experiments is directed toward the head of PDC. The average velocity for the station-keeping glider was 10.78 and 10.96 cm/s for the first and second experiments, respectively. If we take the dominant length scale (the length scale of important physical processes in this system) of PDC to be ~22 km, these velocities suggest that it would take a surface particle approximately 2.27 days to drift from the deepest portion of PDC to Anvers Island. This
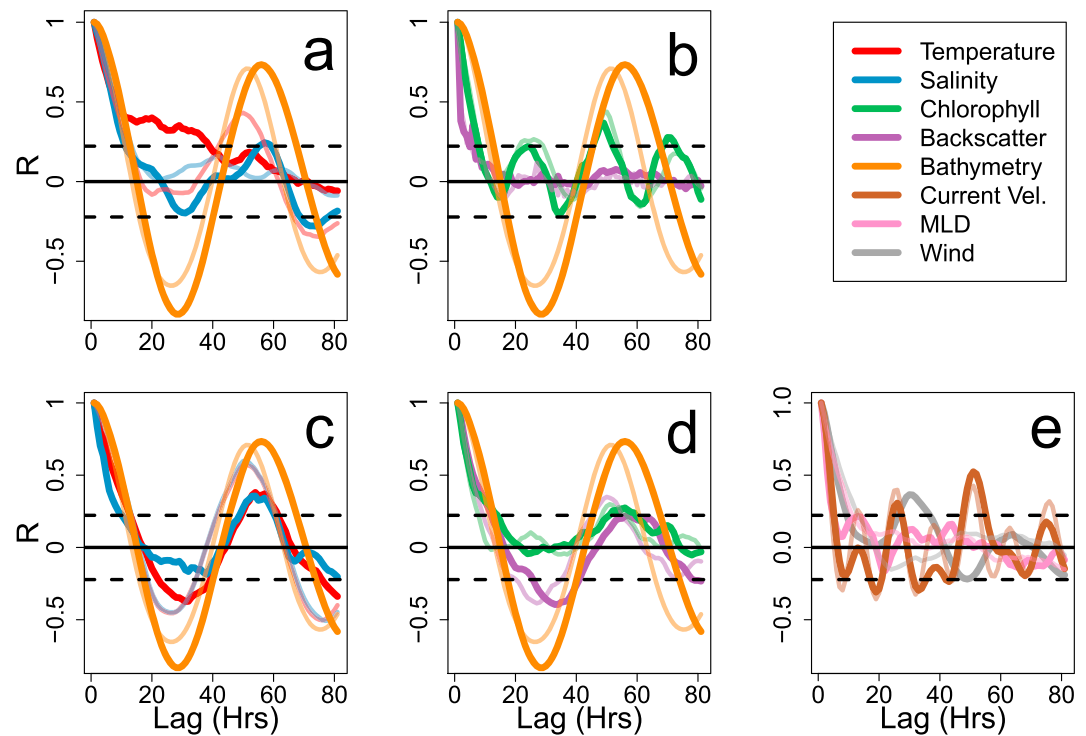
Figure 8. As in Figure 7 except with the along-canyon glider and bathymetry.

time scale is similar to the residence times (~2.1 days) of particles estimated by Kohut et al. (2018). Using the same length scale, the along- and across-canyon gliders have similar mean residence times (Figure S12).
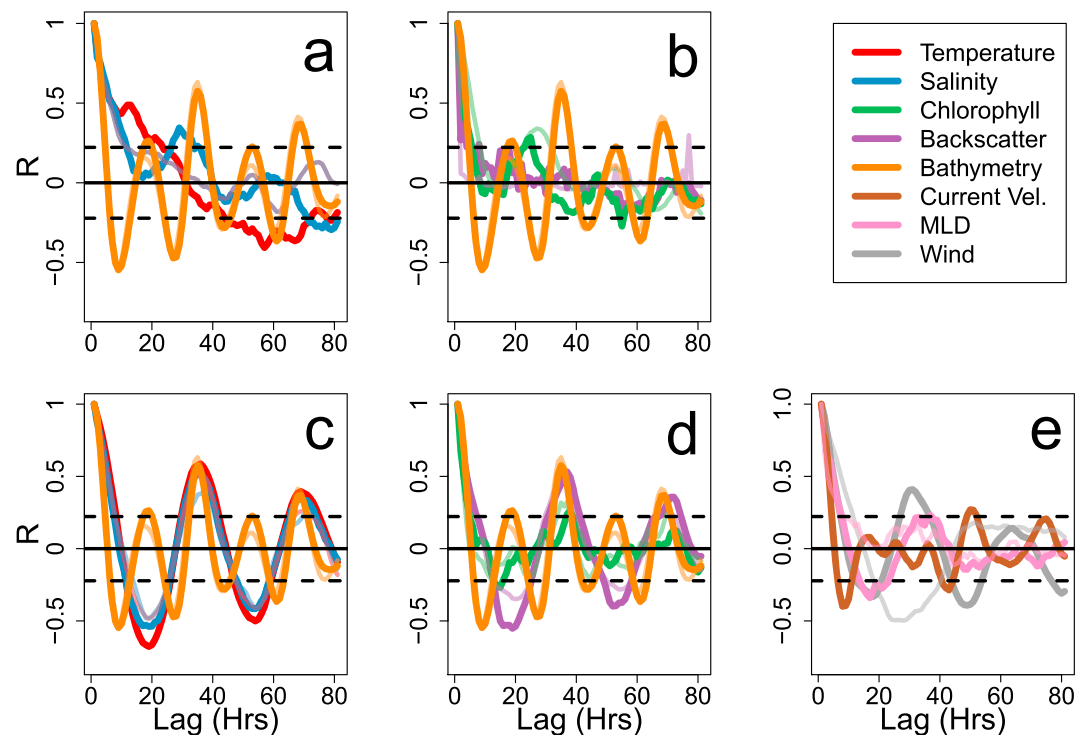
3.2. Decorrelation Analysis

Decorrelation analysis was used to separate time and space variabilities across the canyon. Decorrelation time scales in the station-keeping glider were used to represent variability in time, while differences between the station-keeping and the along- and across-canyon gliders were used to represent spatial variability. If mUCDW upwelling, or any influence of subsurface water masses on surface waters, was present, we expect to see spatial variability in the surface layers over the canyon with similar periods to the underlying canyon bathymetry.

The decorrelation time scales observed by all three gliders are presented in Table 1. In the sections below, we highlight results and patterns that are relevant to our hypothesis.

3.2.1. Station-Keeping Glider Decorrelation Analysis

In the surface layer, the station-keeping glider observed decorrelation scales between 5 (backscatter) and 25 (temperature) hr during the first experiment (Figures 7a and 7b and Table 1). In the second experiment, temperature decorrelated at 50 hr (Figure 7a and Table 1). This is likely due to more uniform temperature in the surface layer in the second half of the season (Figure 2b). The only property that recorrelated in this surface layer was chlorophyll at lags of 24, 50, and 72 hr (Figure 7b). Backscatter, however, did not show these patterns (Figure 7b). Therefore, the decorrelation pattern in chlorophyll is likely due to daily NPQ cycles and not changes in biomass. There were similar patterns in chlorophyll and backscatter during the second experiment (Figure 7b).

At depth, decorrelation time scales ranged between 10 (temperature and salinity) and 15 (chlorophyll and backscatter; Table 1). Again, temperature and salinity decorrelation time scales increased to 40 hr in the second experiment, due to more uniform temperature and salinity properties at depth as the season progressed (Figures 2c and S2b). Optical properties decorrelated at similar time scales in the second experiment.

Figure 9. As in Figure 7 except with the across-canyon glider and bathymetry.

Current velocities decorrelated and recorrelated at periodicities consistent with tidal periods in PDC (Figure 7e).

3.2.2. Along- and Across-Canyon Decorrelation Analyses

The along- and across-canyon glider time series include signals from PDC changing in time and in space. Therefore, we included the decorrelation of bathymetry, which only changes in space along the glider track as a reference for the along- and across-canyon decorrelation analyses (Figures 8 and 9). The bathymetry for the along-canyon glider has maximum anticorrelation at 28 hr and maximum recorrelation at 55 hr. This corresponds to the average velocity of the along-canyon glider of 0.496 km/hr and represents the time it takes the along-canyon glider to travel offshore (anticorrelate) and then return onshore (recorrelate).

In surface waters along PDC, decorrelation time scales ranged from 5 (chlorophyll and backscatter) to 40 (temperature) hr (Figures 8a and 8b and Table 1). Decorrelation time scales were similar in the second experiment and temperature decorrelation time scales decreased to 15 hr (Figure 8a and Table 1). Temperature in the second experiment also recorrelated around 50 hr, which was similar to the recorrelation time scales of bathymetry. This is likely due to increased temperatures over shallower portions of the canyon (Figure 2c). Chlorophyll recorrelated approximately every 24 hr, likely reflecting NPQ (Figure 8b). Across all measured variables in the surface layer, with the exception of temperature recorrelation patterns in the second experiment, there was little to no coherence between the decorrelation scales of the measured variables and the decorrelation scale of the bathymetry (Figures 8a and 8b).

At depth, decorrelation time scales ranged from 10 to 15 hr across physical and optical properties (Table 1). Temperature anticorrelated at 30 hr, and both temperature and salinity recorrelated at 50 hr (Figure 8c). These correspond to the bathymetry decorrelations (Figure 8c). A similar pattern was observed in the chlorophyll and backscatter concentrations, although it was more pronounced in backscatter than chlorophyll, with backscatter anticorrelating at 32 hr and both backscatter and chlorophyll recorrelating at 55 hr (Figure 8d).

Since the along-canyon transect was the only transect to be sampled continuously through both experiments, we performed decorrelation analysis on the continuous time series (Figure S13). The decorrelation scales for the continuous time series are similar to those in the two experiments, with the exception of

temperature and salinity above the mixed layer, and MLD (Figures S13a and S13e). We attribute these differences to gradual seasonal changes that occur within the continuous time series on greater temporal scales than the lag scales examined. Temperature, salinity, and backscatter below the mixed layer continued to correspond with bathymetry correlations (Figures S13c and S13d).

The bathymetry of the across-canyon glider transitioned from shallow, then to deep, and back to shallow as it traversed the canyon from one flank to the other. Therefore, the first recorrelation at 20 hr in the across-canyon glider represents a single crossing, and the second recorrelation at 35 represents the return trip to the original location, which corresponds to an average glider velocity of 0.604 km/hr.

In the surface, decorrelation time scales ranged between 2.5 (backscatter) and 25 (temperature) hr (Figures 9a and 9b and Table 1). Salinity recorrelated at 28 hr and temperature anticorrelated at 57 hr (Figure 9a). Chlorophyll recorrelated at 24 hr (Figure 9b). Similar patterns were observed in the second experiment (Figures 9a and 9b). However, there was no obvious relationship between these decorrelations and the bathymetry decorrelation scale (Figures 9a and 9b).

At depth, temperature, salinity, and backscatter showed similar decorrelation patterns, with these variables decorrelating at 8 hr and exhibiting recorrelations at 35 and 68 hr and anticorrelations at 18 and 53 hr (Figures 9c and 9d). The decorrelation patterns in bathymetry are approximately twice the frequency of the decorrelation patterns in the temperature, salinity, and backscatter of deeper water masses. This suggests that the changes in these properties are only associated with one side of PDC at depth. This pattern was also reflected in the time series and average across-canyon transects (Figures 2d, 3c, 4d, S6, and S7).

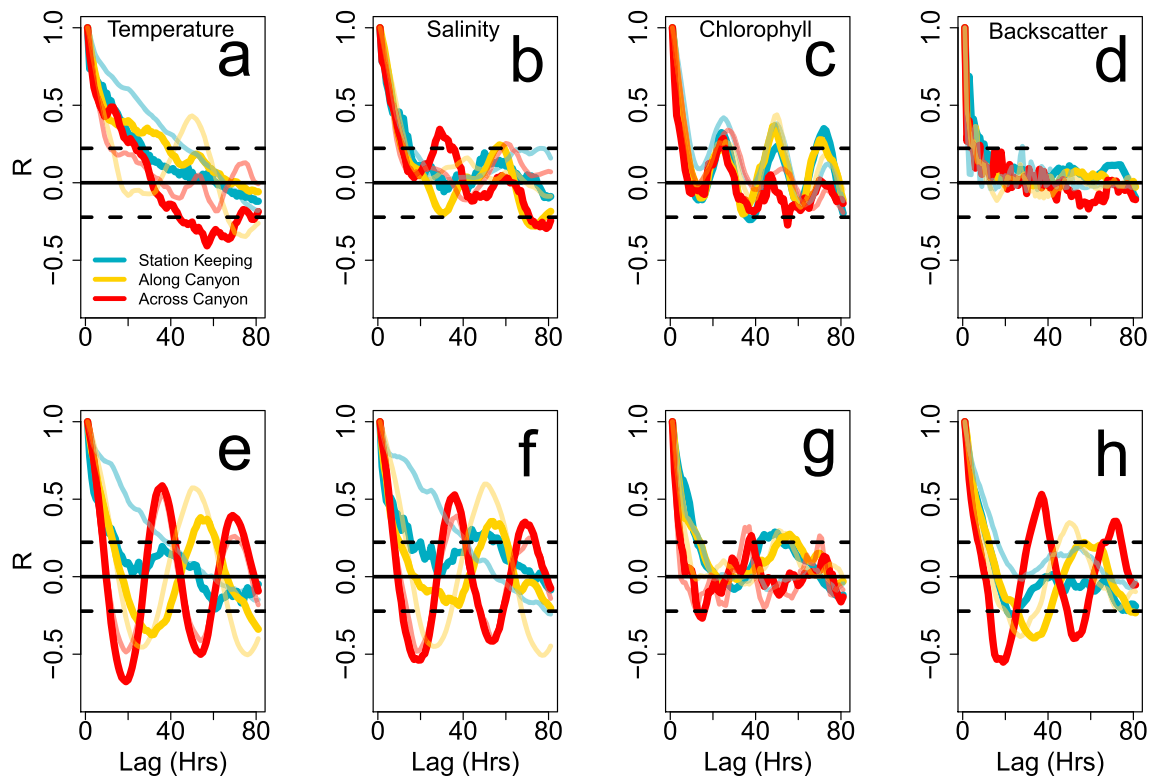### 3.2.3. Comparison of Decorrelations

The decorrelation analysis of waters between 0–10 and 80–90 m shows that shallow water dynamics differ from those observed in deeper waters (Figures 7–10). In the surface layer, salinity, chlorophyll, and backscatter decorrelated rapidly on similar time scales (Figures 10a and 10d and Table 1) irrespective of glider movements, indicating that the surface layer is not spatially structured as we would expect in a persistent bathymetry-related upwelling scenario (Figures 8a, 8b, 9a, and 9b). At depth, decorrelation time scales were dissimilar across all three gliders (Figures 10e, 10f, and 10h). Recorrelations in the along- and across-canyon gliders were similar to the recorrelation patterns of canyon bathymetry (Figures 8, 9c, and 9d).

3.3. Historical Palmer LTER Nutrient and Light Profiles

Historical macronutrient profiles from the Palmer LTER indicate that nutrients within the surface mixed layer are not limiting within PDC nor along the nearby continental shelf. In PDC, surface phosphate ranges from approximately 1.5 to 1.75 μmol/L from the surface to 25 m, which was the depth of WW according to our definitions in the mean temperature and salinity profiles (Figure S2a). Over these depths, silicate concentrations range between 60 and 72 μmol/L and nitrate concentrations range between 20 and 25 μmol/L (Figure S2a). On the continental shelf, similar nutrient concentrations were observed (Figure S2b). Phosphate concentrations were ~1.5 μmol/L, silicate concentrations ranged between ~57 and 80 μmol/L, and nitrate concentrations were ~20 μmol/L between the surface and 25 m (Figure S2b). These nutrient concentrations are relatively stable in the WW and increase with depth in the mUCDW (Figure S2). While nitrate and phosphorus are rarely limiting in the WAP (Smith et al., 1996), nitrate and phosphorus have been shown to be limiting in nearshore regions at ~2 and below 0.02 μmol/L, respectively (Holm-Hanson et al., 1989). Silicate has been shown to be limiting below 5 μmol/L (Nelson et al., 2001). Light irradiance decreased exponentially with depth (Figure S14). The 1% and 5% light level was on average 46.9 ± 17.1 and 24.8 ± 6.5 m, respectively (Figure S14).

4. Discussion

For localized upwelling of mUCDW to act as the mechanism maintaining the biological hotspot, it must reach a lighted, nutrient-limited surface layer and be retained long enough to affect phytoplankton abundance through growth. Satellite observations of increased chlorophyll over PDC provide a strong circumstantial case for this view (Kavanaugh et al., 2015). However, we believe that our analysis suggests (1) that upwelling of mUCDW into the surface layer is not the dominant physical signal, (2) that the surface layer is neither macronutrient nor micronutrient limited, and (3) that the surface residence times are too short for phytoplankton growth rates respond to any upwelling event.

Figure 10. Comparisons of the decorrelation scales of temperature (a,e), salinity (b,f), chlorophyll (c,g), and backscatter (d,h) decorrelations in the surface (0–10 m; a–d) and deep layers (80–90 m; e–h) between the stationary, along-canyon, and across-canyon gliders. Solid lines represent decorrelations during the first experiment, and translucent lines represent decorrelations during the second experiment. Dashed lines represent the 95% confidence intervals of zero correlation.

We observed no obvious entrainment of mUCDW into the mixed layer throughout PDC. The mUCDW was separated from AASW by a layer of WW (Figure 3). Although we observed spatial differences in the depth of mUCDW (Figures S5–S8), WW persisted as a boundary between the surface waters and mUCDW (Figure 3). Furthermore, the three gliders showed similar decorrelation patterns in AASW despite spatial differences in glider transects (Figures 10a–10d). These patterns were not similar to the decorrelation patterns in the canyon bathymetry, suggesting that there is no canyon effect within the surface mixed layer. This is contrary to our hypothesis that surface decorrelation patterns would be similar to canyon bathymetry if canyon-driven upwelling was occurring within PDC (Figures 8–10).

Ship-based observations from 1993 to 2018 in the Palmer LTER suggest that our observations are typical for this system during the austral summer. WW was present in 87.5% of CTD casts at Station 600-040 and was between 36- and 51-m depth during these casts, consistent with our observations (Figures 3 and S6–S9). In addition, mUCDW was found in 93.8% of profiles below 86 m, which was similar to our observations (Figures 3 and S6–S9) and consistent with six seasons of glider observations within the austral summer in PDC (Carvalho et al., 2016). Nutrient profiles from this historical data set also suggest that this system is not nutrient limited. Macronutrients nitrogen, phosphorous, and silica were abundant in the upper 20 m of the water column within PDC and along the continental shelf (Figure S2).

While these nutrient profiles do not indicate upwelling, it is possible that nutrients are supplied to the surface via diffusive fluxes from mUCDW. Recent studies along the WAP suggest diffusive fluxes play a vital role to local nutrient dynamics (Bown et al., 2018; Henley et al., 2018; Pedulli et al., 2014), so this is a possible mechanism for mUCDW to influence surface productivity. It is also possible that while the Palmer LTER data set analyzed has high temporal resolution across years (i.e. 1993–2018), these observations are spatially and seasonally limited since these sampling events only occur in January or early February each year. Therefore, the Palmer LTER data may miss upwelling events that possibly occurred earlier or later in the season or at different locations within PDC. The data also could not resolve pulsed nutrient supplies, or short

periods of nutrient limitation (Henley et al., 2017; Henley et al., 2018; Kim et al., 2016), that could have a significant impact on regional productivity.

Recent observations show that iron, a critical micronutrient, is not primarily sourced from mUCDW upwelling but from nearby glacial and sediment runoff (Sherrell et al., 2018). Therefore, if mUCDW was upwelling, it would likely not have an effect on phytoplankton growth. This agrees with field incubation experiments (Carvalho et al., 2019). Furthermore, light irradiance data show that the 1% light level (depth of the euphotic zone) in PDC is on average 47 m during the summer months (Figure S14). mUCDW is not found at these depths until stratification begins to break down late in the growing season.

Beyond the lack of an upwelling signal and nutrient limitation, it is likely that surface water residence time over PDC is too short to attribute high phytoplankton biomass to local growth driven by localized upwelling. The residence time of surface waters based on simulated drifters (Kohut et al., 2018) and integrated glider currents (Figure 6 and S12) is ~2.2 days, while the doubling time of phytoplankton in this region is on the order of ~7 to ~70 days (Moline, 1996). Growth rate estimates based on chlorophyll concentrations measured annually in Ryder Bay, south of PDC, since 1998 suggests the doubling time is ~100 days, assuming exponential growth (Venables et al., 2013). This suggests that if mUCDW is upwelling and was systematically missed by glider observations, it would be quickly transported away. These low residence times could also explain why the salinity, chlorophyll, and backscatter decorrelation patterns in the surface between the three gliders are similar despite the difference in the glider locations relative to each other (Figures 10a–10d).

If local upwelling is not the mechanism maintaining the biological hotspot, then there must be another mechanism driving this phenomenon. Below, we attempt to reconcile satellite observations of enhanced phytoplankton biomass from Kavanaugh et al. (2015) over PDC (section 4.1) and then propose testable alternative hypotheses to account for the hotspot phenomenon in PDC (section 4.2).

4.1. Reconciling Satellite Observations

Satellite observations of lower ice and higher chlorophyll concentrations over PDC provided strong circumstantial evidence for local upwelling and retention of warm mUCDW (Kavanaugh et al., 2015). However, the lack of a clear upwelling signal of mUCDW (Figure 3) calls this interpretation into question. It is possible there is episodic upwelling over the canyon where the gliders did not sample. For example, mUCDW could be upwelling over portions of the eastern flank of PDC that were not sampled by the across-canyon glider where mUCDW was high in the water column and were therefore missed here. Whether or not local upwelling is ecologically relevant depends both on surface residence times that are longer than the phytoplankton growth rate and that the phytoplankton are nutrient limited. Neither of these appear to be true. In addition, mUCDW does not transfer heat to the surface mixed layer as proposed by Kavanaugh et al. (2015), due to WW acting as a barrier to heat transfer to the surface (Figure 3).

Rather than upwelling of warm mUCDW melting sea ice, the lack of sea ice observed by Kavanaugh et al. (2015) over PDC could be attributed to strong surface currents or local winds. Notably, Kavanaugh et al. (2015) did not observe a temperature difference between canyon and noncanyon sites in PDC, suggesting that there could be other mechanisms creating low-ice conditions. Other coastal canyons along the WAP have also been associated with ice-free regions (Schofield et al., 2013) that are coupled with significant increases in productivity due to increased irradiance (Smith & Gordon, 1997), suggesting that these systems are light limited rather than nutrient limited. It is important to note that observations in PDC may not apply to the other canyon systems examined by Kavanaugh et al. (2015) because the Bismark Strait provides a conduit for flow away from the canyon (Figure 1).

4.2. Horizontal Transport as a Potential Hotspot Supporting Mechanism

The short surface residence time in PDC (this study; Kohut et al., 2018) strongly suggest that enhanced phytoplankton and krill biomass is a result of the advection of high concentrations of phytoplankton and krill biomass from the continental shelf into PDC, rather than local production of biomass supported by local upwelling, as suggested by the canyon hypothesis. However, it is unknown what these transport mechanisms are or how they interact with PDC.

There is evidence of isopycnal doming over the deepest parts of the canyon (Figures 3b, S4c, and S15). If we take these sloping isopycnals indicate doming within PDC, this doming may be associated with stretching of

the water column as water moves over the canyon through conservation of potential vorticity, leading to the uplift of the denser waters in the middle of the canyon (Klinck, 1989; Mackas et al., 1997). One possibility that would explain isopycnal doming and the strong coherence between bathymetry, temperature, and salinity (Figures 8c, 8d, 9c, 9d, and 10e–10h) below the mixed layer would be the presence of a subsurface recirculating eddy over the canyon (Allen & Hickey, 2010). Sloping isopycnals over the canyon generate a geostrophically balanced pressure gradient leading to the formation of an eddy around the rim of the canyon (Allen et al., 2001). Based on mean density profiles from Station 600-040 and a maximum glider sampling depth of 200 m, an internal radius of deformation below the mixed layer was estimated as ~7.5 km. Since the moving gliders had transects approximately 20 km long both along and across PDC, it is possible that we observed subsurface geostrophic flows. Although speculative, this may explain why the decorrelation scales of deep backscatter are coherent with bathymetry in PDC (Figures 8 and 9). Analysis of modeled drifters released within PDC suggests that residence time below the mixed layer (~50 m) is approximately 25 days (Couto, Kohut, et al., 2017), possibly allowing these waters to accumulate particles exported from the surface layer.

While it is possible that a recirculating eddy within PDC is facilitating the accumulation of particles, the nature of these high backscatter returns is unknown. Since these particles were observed far from shore over the deepest portions of the canyon, we propose that they are more likely to be biogenic than terrigenous. They do not exhibit correlations to chlorophyll fluorescence nor do they perform diurnal vertical migration (Goodrich, 2018; Figure S16). Therefore, it is possible that these particles may be aggregates of organic material that are caught in a deep recirculation pattern over PDC. Whether or not this hypothesized recirculation feature has any impact on larger zooplankton, and by extension, zooplankton predators is unknown. Krill have high diurnal vertical directed swimming speeds and could vertically migrate out this retentive feature. However, if krill horizontal movement is undirected and random, they could be retained by a coherent deep recirculating flow during the day.

There are several key assumptions that need to be tested if a deep recirculation pattern could serve as a mechanistic explanation for the canyon hypothesis: The (1) particles have a higher residence time at depth compared to the surface; (2) krill, like these particles, are retained in the deep portions of the canyon; and (3) vertically migrate to the surface layers where they are (4) accessible by predators via horizontal transport in the surface layer.

References

Allen, S. E., & Hickey, B. M. (2010). Dynamics of advection-driven upwelling over a shelf break submarine canyon. *Journal of Geophysical Research*, *115*, C05008. https://doi.org/10.1029/2009JC005731

Allen, S. E., Vindeirinho, C., Thomson, R. E., Foreman, M. G. G., & Mackas, D. L. (2001). Physical and biological processes over a submarine canyon during an upwelling event. *Canadian Journal of Fisheries and Aquatic Sciences*, *58*(4), 671–684. https://doi.org/10.1139/cjfas-58-4-671

Bown, J., van Haren, H., Meredith, M. P., Venables, H. J., Laan, P., Brearley, J. A., & de Baar, H. J. (2018). Evidences of strong sources of DFe and DMn in Ryder Bay, Western Antarctic Peninsula. *Philosophical Transactions of the Royal Society A: Mathematical, Physical and Engineering Sciences*, *376*, 2122. https://doi.org/10.1098/rsta.2017.0172

Carvalho, F., Fitzsimmons, J., Couto, N., Waite, N., Gorbunov, M., Kohut, J., et al. (2019), Testing the canyon hypothesis: Evaluating light and nutrient controls of phytoplankton growth in penguin foraging hotspots along the West Antarctic Peninsula. *Limnology and Oceanography*. https://doi.org/10.1002/LNO.11313

Carvalho, F., Kohut, J., Oliver, M. J., & Schofield, O. (2017). Defining the ecologically relevant mixed-layer depth for Antarctica's coastal seas. *Geophysical Research Letters*, *44*, 338–345. https://doi.org/10.1002/2016GL071205

Carvalho, F., Kohut, J., Oliver, M. J., Sherrell, R. M., & Schofield, O. (2016). Mixing and phytoplankton dynamics in a submarine canyon in the West Antarctic Peninsula. *Journal of Geophysical Research: Oceans*, *121*, 5069–5083. https://doi.org/10.1002/2016JC011650

Couto, N., Kohut, J., Schofield, O., Dinniman, M. & Graham, J. (2017). Pathways and retention times in a biologically productive canyon system on the West Antarctic Peninsula. In *OCEANS–Anchorage, 2017*, 1-8. IEEE.

Couto, N., Martinson, D. G., Kohut, J., & Schofield, O. (2017). Distribution of Upper Circumpolar Deep Water on the warming continental shelf of the West Antarctic Peninsula. *Journal of Geophysical Research: Oceans*, *122*, 5306–5315. https://doi.org/10.1002/2017JC012840

Ducklow H., Vernet M., & Prezelin B. (2019). Dissolved inorganic nutrients including 5 macro nutrients: Silicate, phosphate, nitrate, nitrite, and ammonium from water column bottle samples collected during annual cruise along western Antarctic Peninsula, 1991–2018. *Environmental Data Initiative*. https://doi.org/10.6073/pasta/29e7035681f2496a78f097fd2fcb6ce0

Emslie, S. D., & Patterson, W. P. (2007). Abrupt recent shift in δ^{13}C and δ^{15}N values in Adélie penguin eggshell in Antarctica. *PNAS*, *104*(28), 11,666–11,669. https://doi.org/10.1073/pnas.0608477104

Fraser, W. R., & Trivelpiece, W. Z. (1996). Factors controlling the distribution of seabirds: Winter-summer heterogeneity in the distribution of Adelie penguin populations. *Antarctic Research Series*, *70*, 257–272. https://doi.org/10.1029/AR070p0257

Goodrich, C. S. (2018). Sustained glider observations of acoustic scattering suggest zooplankton patches are driven by vertical migration and surface advective features in Palmer Canyon, Antarctica. Master's Thesis, University of Delaware.

Henley, S. F., Jones, E. J., Venables, H. J., Meredith, M. P., Firing, Y. L., Dittrich, R., et al. (2018). Macronutrient and carbon supply, uptake and cycling across the Antarctic Peninsula shelf during summer. *Philosophical Transactions of the Royal Society a-Mathematical Physical and Engineering Sciences*, *376*(2122), 20170168. https://doi.org/10.1098/rsta.2017.0168

Henley, S. F., Tuerena, R. E., Annett, A. L., Fallick, A. E., Meredith, M. P., Venables, H. J., et al. (2017). Macronutrient supply, uptake and recycling in the coastal ocean of the west Antarctic Peninsula. *Deep-Sea Research Part II-Topical Studies in Oceanography*, *139*, 58–76. https://doi.org/10.1016/j.dsr2.2016.10.003

Holm-Hanson, O., Mitchell, B. G., Hewes, C. D., & Karl, D. M. (1989). Phytoplankton blooms in the vicinity of palmer station, Antarctica. *Polar Biology*, *10*(1), 49–57. https://doi.org/10.1007/BF00238290

Iannuzzi, R. (2018). Conductivity Temperature Depth (CTD) sensor profile data binned by depth from PAL LTER annual cruises, 1991–2017 (ongoing). *Environmental Data Initiative*. https://doi.org/10.6073/pasta/12276fbc0d68568177702aed0d4b44bc

Kavanaugh, M. T., Abdala, F. N., Ducklow, H., Glover, D., Fraser, W., Martinson, D., et al. (2015). Effect of continental shelf canyons on phytoplankton biomass and community composition along the western Antarctic Peninsula. *Marine Ecology Progress Series*, *524*, 11–26. https://doi.org/10.3354/meps11189

Kim, H., Doney, S. C., Iannuzzi, R. A., Meredith, M. P., Martinson, D. G., & Ducklow, H. W. (2016). Climate forcing for dynamics of dissolved inorganic nutrients at Palmer Station, Antarctica: An interdecadal (1993–2013) analysis. *Journal of Geophysical Research: Biogeosciences*, *121*, 2369–2389. https://doi.org/10.1002/2015JG003311

Klinck, J. M. (1989). Geostrophic adjustment over submarine canyons. *Journal of Geophysical Research*, *94*(C5), 6133–6144. https://doi.org/10.1029/JC094iC05p06133

Kohut, J., Bernard, K., Fraser, W., Oliver, M. J., Statscewich, H., Winsor, P., & Miles, T. (2014). Studying the impacts of local oceanographic processes on Adélie penguin foraging ecology. *Marine Technology Society Journal*, *48*(5), 25–34. https://doi.org/10.4031/MTSJ.48.5.10

Kohut, J. T., Winsor, P., Statscewich, H., Oliver, M. J., Redj, E., Couto, N., et al. (2018). Variability in summer surface residence time within a West Antarctic Peninsula biological hotspot. *Philosophical Transactions of the Royal Society A*, *376*(2122), 20170165. https://doi.org/10.1098/rsta.2017.0165

Mackas, D. L., Kieser, R., Saunders, M., Yelland, D. R., Brown, R. M., & Moore, D. F. (1997). Aggregation of euphausiids and Pacific hake (*Merluccius productus*) along the outer continental shelf off Vancouver Island. *Canadian Journal of Fisheries and Aquatic Sciences*, *54*(9), 2080–2096. https://doi.org/10.1139/f97-113

McDougall, T. J., & Krzysik, O. A. (2015). Spiciness. *Journal of Marine Research*, *73*(5), 141–152. https://doi.org/10.1357/002224015816665589

Moline, M. A. (1996). Temporal dynamics and regulation of coastal Antarctic phytoplankton communities: Spring/summer 1991–1994. Doctoral Dissertation, University of California, Santa Barbara.

Nelson, D. M., Brzezinski, M. A., Sigmon, D. E., & Franck, V. M. (2001). A seasonal progression of Si limitation in the Pacific sector of the Southern Ocean. *Deep Sea Research Part II: Topical Studies in Oceanography*, *48*(19-20), 3973–3995. https://doi.org/10.1016/S0967-0645(01)00076-5

Oliver, M. J., Irwin, A., Moline, M. A., Fraser, W., Patterson, D., Schofield, O., & Kohut, J. (2013). Adélie penguin foraging location predicted by tidal regime switching. *PLoS ONE*, *8*(1), e55163. https://doi.org/10.1371/journal.pone.0055163

Oliver, M. J., Kohut, J. T., Bernard, K., Fraser, W., Winsor, P., Statscewich, H., et al. (2019). Central place foragers select ocean surface convergent features despite differing foraging strategies. *Scientific Reports*, *9*, 157. https://doi.org/10.1038/s41598-018-35901-7

Pedulli, M., Bisagni, J. J., Ducklow, H. W., Beardsley, R., & Pilskaln, C. (2014). Estimates of potential new production (PNP) for the waters off the western Antarctic Peninsula (WAP) region. *Continental Shelf Research*, *84*, 54–69. https://doi.org/10.1016/j.csr.2014.05.011

Pickett, E. P., Fraser, W. R., Patterson-Fraser, D. L., Cimino, M. A., Torres, L. G., & Friedlaender, A. S. (2018). Spatial niche partitioning may promote coexistence of *Pygoscelis* penguins as climate-induced sympatry occurs. *Ecology and Evolution*, *8*(19), 9764–9778. https://doi.org/10.1002/ece3.4445

Prézelin, B. B., Hofmann, E. E., Mengelt, C., & Klinck, J. M. (2000). The linkage between Upper Circumpolar Deep Water (UCDW) and phytoplankton assemblages on the west Antarctic Peninsula continental shelf. *Journal of Marine Research*, *58*(2), 165–202. https://doi.org/10.1357/002224000321511133

R Core Team (2017). R: A language and environment for statistical computing. R Foundation for Statistical Computing, Vienna, Austria. URL https://www.R-project.org/.

Ryan, W. B. F., Carbotte, S. M., Coplan, J., O'Hara, S., Melkonian, A., Arko, R., et al. (2009). Global Multi-Resolution Topography (GMRT) synthesis data set. *Geochemistry, Geophysics, Geosystems*, *10*, Q03014. https://doi.org/10.1029/2008GC002332

Schmitt, R. W. (1999). Spice and the demon. *Science*, *283*(5401), 498–499. https://doi.org/10.1126/science.283.5401.498

Schofield, O., Ducklow, H., Bernard, K., Doney, S., Patterson-Fraser, D., Gorman, K., et al. (2013). Penguin biogeography along the West Antarctic Peninsula: Testing the canyon hypothesis with Palmer LTER observations. *Oceanography*, *26*(3), 204–206. https://doi.org/10.5670/oceanog.2013.63

Schofield, O., Kohut, J., Aragon, D., Creed, L., Graver, J., Haldeman, C., et al. (2007). Slocum gliders: Robust and ready. *Journal of Field Robotics*, *24*(6), 473–485. https://doi.org/10.1002/rob.20200

Sherrell, R. M., Annett, A. L., Fitzsimmons, J. N., Roccanova, V. J., & Meredith, M. P. (2018). A 'shallow bathtub ring' of local sedimentary iron input maintains the Palmer Canyon biological hotspot on the West Antarctic Peninsula shelf. *Philosophical Transactions of the Royal Society A*, *376*, 20170171. https://doi.org/10.1098/rsta.2017.0171

Smith, D. A., Hofmann, E. E., Klinck, J. M., & Lascara, C. M. (1999). Hydrography and circulation of the west Antarctic Peninsula continental shelf. *Deep Sea Research Part I: Oceanographic Research Papers*, *46*(6), 925–949. https://doi.org/10.1016/S0967-0637(98)00103-4

Smith, W. O. Jr., & Gordon, L. I. (1997). Hyperproductivity of the Ross Sea (Antarctica) polynya during the austral spring. *Geophysical Research Letters*, *24*(3), 233–236. https://doi.org/10.1029/96GL03926

Smith, W. O. Jr., Nelson, D. M., DiTullio, G. R., & Leventer, A. R. (1996). Temporal and spatial patterns in the Ross Sea: Phytoplankton biomass, elemental composition, productivity and growth rates. *Journal of Geophysical Research*, *101*(C8), 18,455–18,465. https://doi.org/10.1029/96JC01304

Venables, H. J., Clarke, A., & Meredith, M. P. (2013). Wintertime controls on summer stratification and productivity at the western Antarctic Peninsula. *Limnology and Oceanography*, *58*(3), 1035–1047. https://doi.org/10.4319/lo.2013.58.3.1035